ECS Transactions, 78 (1) 807-815 (2017)
10.1149/07801.0807ecst ©The Electrochemical Society

Influence of the Bias Substrate Power on the GDC Buffer Layer

E. Breaz[a,b,c], E. Aubry[a], A. Billard[a,b], N. Coton[d] , P. Coquoz[d], A. Pappas[d], S. Diethelm[e]
R. Ihringer[d] and P. Briois[a,b]

[a]FEMTO-ST Institute UMR 6174, CNRS, Univ. Bourgogne Franche-Comté, UTBM
F-90010 Belfort, France
[b]FC Lab Research (FR CNRS 3539), Rue Thierry Mieg, F-90010 Belfort, France
[c]Department of Electrical Engineering, Technical University of Cluj-Napoca
Cluj-Napoca, Romania
[d]Fiaxell Sàrl, PSE A, Science Park, 1015 Lausanne, Switzerland
[e]Ecole Polytechnique Fédérale de Lausanne (EPFL), 1015 Lausanne, Switzerland

Gadolinia Doped Ceria (GDC) buffer layers were synthesized by reactive magnetron sputtering under different bias powers applied to the substrate holder. All as-deposited coating present a face centered cubic (f.c.c) structure of ceria with dense and adhesive morphology. Only the film deposited under 80 W bias power applied to the substrate does not exhibit cracks after an annealing treatment during 2 h under air at 1000°C. The performance of the cell is 670 $mW.cm^{-2}$ @ 800 $mA.cm^{-2}$ at 790°C and no degradation was observed after 150 hours.

Introduction

Nowadays, regarding the SOFC (Solid Oxide Fuel Cell) technology, it is necessary to decrease the operating temperature to 700°C (650-750°C) of IT-SOFC technology, which currently is around 850-900°C for electrolyte supported cell used by the three main operators – Bloom, Hexis and Sun Fire. At this temperature, the reactivity and the components cost of the cell decrease [1]. Nevertheless, some interactions between the conventional electrolyte material (YSZ) and the cathode material (lanthanum based) are still present and it is necessary to include a ceria buffer layer to avoid the possible formation of an insulating pyrochlore structure $La_2Zr_2O_7$ layer at the electrolyte-cathode interface [2-3]. In ceria family, the best material regarding the ionic conductivity is the samaria doped ceria. However, the gadolinia doped ceria (GDC) is the most employed from the cost point of view and the availability of gadolinium in comparison with samarium [4]. This buffer layer avoids the reactivity between electrolyte and cathode, and presents a good anionic conductivity. It must be dense, thin and adhesive on electrolyte, in order to be suitable for the surface treatment process [3].

In this paper, we present some recent results obtained on GDC coatings deposited by magnetron sputtering from metallic targets in argon-oxygen reactive gas mixtures with different substrate bias powers. The targeted thickness is around 1 µm. First, the experimental device will be introduced, followed by the chemical, microstructural and structural characterization (SEM, XRD,…) of the GDC coatings in relation with the magnetron sputtering deposition parameters. From the buffer layers obtained, the best one have been choosen in order to perform a complete cell test (Ni-

YSZ/YSZ/GDC/LSCF) on the Fiaxell Open Flanges set up. The results and the discussions of the cell test are presented at the end followed by the conclusions.

Experimental Details

Sputtering Device for GDC Buffer Layer Elaboration

The experimental device is a 100-litre Alcatel SCM 650 sputtering chamber pumped down via a system combining XDS35i Dry Pump and a 5401CP turbo-molecular pump. The sputtering chamber is equipped with three 200 mm diameter magnetron targets and with a 620 mm diameter rotating substrate holder parallel to the targets at a distance of about 110 mm. The distance between the targets axis and that of the substrate holder is 170 mm. The Ce-10 at.% Gd target is supplied thanks to a pulsed DC Advanced Energy dual generator allowing the control of the discharge current, power or voltage. In the present study, the discharge current is fixed to 2.5 A. The substrates are glass slide and 2R-Cell produced by Fiaxell. More details concerning the synthesis can be found in a previous work [5]. All the substrates are placed next to the target at 170 mm from the axis of the substrate holder. The argon and oxygen flow rates are controlled with MKS flowmeters and the pressure is measured by using a MKS Baratron gauge.

The deposition stage is monitored by using a closed loop control PEM (Plasma Emission Monitoring) system (Figure 1) using optical emission spectroscopy (OES) [6]. The technique is based on the measurement of the optical intensity of the 418.66 nm Ce emission line (I^*_{Ce}) measured on the area close up to the target. The signal is sent via an optical fiber to a Ropper Scientific SpectraPro 500i spectrometer, with a 1200 groove mm^{-2} grating and a photomultiplier tube (Hamamatsu R 636). Then, the information is transferred to a computer where a program developed under Labview® monitors the oxygen flow rate to maintain the selected intensity of the optical signal I^*_{Ce}.

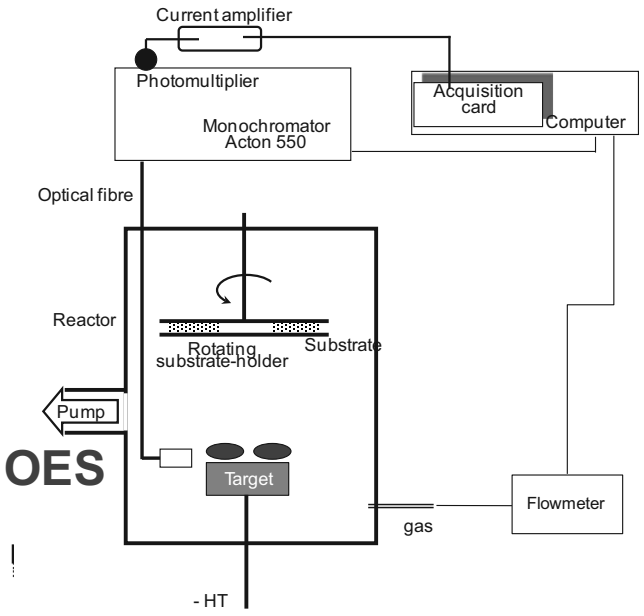

Figure 1. Scheme of Plasma Emission Monitoring system.

Structural and Morphological Characterisation

The structural features of the coatings were performed in Bragg Brentano configuration X-ray diffraction using a BRUKER D8 focus diffractometer ($CoK_{\alpha 1+\alpha 2}$ radiations) equipped with the LynxEye linear detector. Diffractograms were collected under air flow during 10 minutes in the [20°-80°] scattering angle range by steps of 0.019°.

Coating thickness was also determined ex-situ by optical transmittance measurements performed with a UV-visible-NIR Spectrophotometer (UV3600, produced by Shimadzu) using a principle described in [7]. The transmittance curves were fitted by Scout software developed by W. Theiss. These measurements were systematically confirmed by using the step method with an Altysurf profilometer produced by Altimet, which allows an accuracy of around 20 nm. Before each measurement, the calibration of the experimental device was realised with a reference sample number 787569 accredited by CETIM organisation.

The coatings morphology was characterized by Scanning Electron Microscopy (SEM) using a JEOL JSM 7800 F, equipped with Energy Dispersive Spectroscopy (EDS) for chemical measurements.

Electrical Characterisation

A complete current-voltage (I-V) curve has been carried out in the Open Flanges Set-Up, that has been developed and commercialized by Fiaxell Sàrl (Figure 2). This test rig allows a simple and rapid mounting of different size cells, ranging from 20 to 80 mm in diameter, and gives highly reproducible results. The distinctiveness of the Open Flanges Set-Up is that no sealing is required: the SOFC cell is simply squeezed between two alumina felts, and a nickel foam on the anode side and a grid on the cathode side provide current collection. A fuel flow rate between 120 to 200 (ml/min), depending on the cell size, is enough to ensure an OCV (open circuit voltage) close to the theoretical value as have been shown for two different cells. Normal operating conditions are: cell temperature = 790°C, hydrogen flow rate = 100 ml/min, air flow rate= 400 ml/min.

Figure 2. On the left: Drawing of the Open Flange Set-Up developed by Fiaxell. On the right: positioning of the Set-Up in the oven for a measurement.

Results and Discussion

Determination of the Sputtering Parameters

In DC mode, the optical signal of sputtered metal atoms in a pure Ar atmosphere is proportional to the square of the discharge current [8]. By fixing the discharge current of a metallic target, its physicochemical state is usually a monotonic and quite proportional function of the optical signal I^*_M measured by OES [9]. In so called unstable sputtering conditions, i.e. when the oxygen partial pressure - oxygen flow rate curve presents a hysteresis, PEM is a very suitable technique to allow high rate growth of oxide coatings [10]. In this study, the PEM set point of I^*_{Ce} was varied from 40 to 70 % of the obtained signal, while depositing in pure argon atmosphere. Argon flow rate is 50 sccm and no bias voltage is applied. All those deposition conditions take place in the unstable sputtering domain, i.e. where a set point cannot be maintained without using a closed loop control system. As shown in Figure 3, increasing the set point decreases the coating transparency, and then the oxidation rate of the coating. Indeed, the higher is the set point, the higher is the sputtered flow of metal atoms and the the oxygen partial pressure in the reactor is lower. Note that, coatings deposited with a set point of 4 V, i.e. I^*_{Ce} = 40 % correspond to a deposition rate of about 0.8 µm.h^{-1} whereas it is about 0.2 µm.h^{-1} without PEM, i.e. in the so called compound sputtering mode [10]. These deposition conditions are expected to produce fully oxidized GDC coatings. Nonetheless, a further annealing treatment in air for 2 hours at 1000°C was systematically performed to ensure the full oxidation and the good behavior of the coatings at the cathode deposition temperature by screen printing.

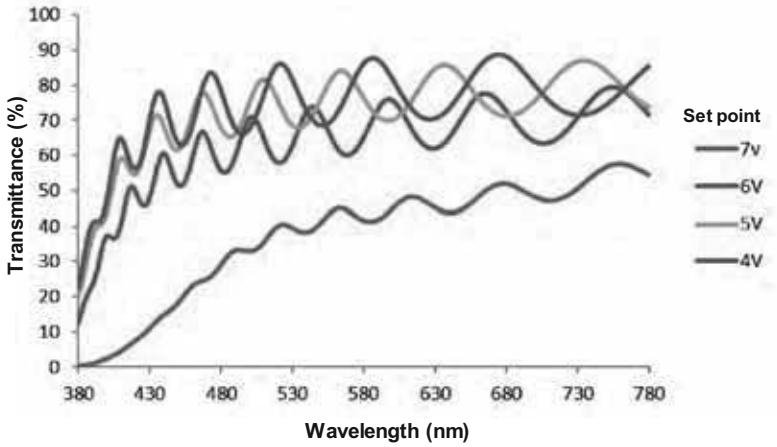

Figure 3. Transmittance on the visible range of GDC coatings deposited with different set points.

Structural and Morphological Characterization

Figure 4 shows the transmittance curve as function of the wavelength for different bias power. The transmittance decreases with the bias power. This phenomenon is induced by the preferential sputtering of oxygen under the effect of the bias power applied on the substrate holder. The coating is less and less transparent and presents a more metallic aspect with the increase of the bias power (Figure 5). The range of coating thickness is from 1.03 to 1.11 µm and it is obtain by fitting the transmittance curve with

the Scout software. These values are close to targeted 1 μm thickness and are confirmed by SEM observations of the brittle fracture cross sections (Figure 6). The observation by SEM of as-deposited coating reveals a relatively dense, adhesive and covering films on the YSZ material for all experiments. After annealing at 1000°C during 2 hours under static air, the SEM observation of the surface presents some cracks for all coatings, except the film synthesized under 80 W substrate bias power. (Figure 7). The polarization increase and the low working pressure (0.5 Pa) allow to generate stress in the coating and during the annealing treatment there is a stress relaxation which avoids cracks occurrence. This behavior is reinforced by the X-ray diffraction patterns with thermal treatment (Figure 8).

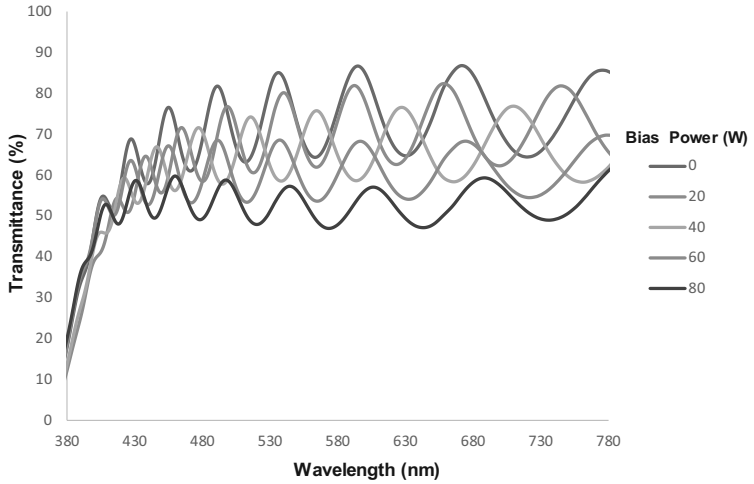

Figure 4. Transmittance on the visible range of GDC coatings deposited with different bias powers.

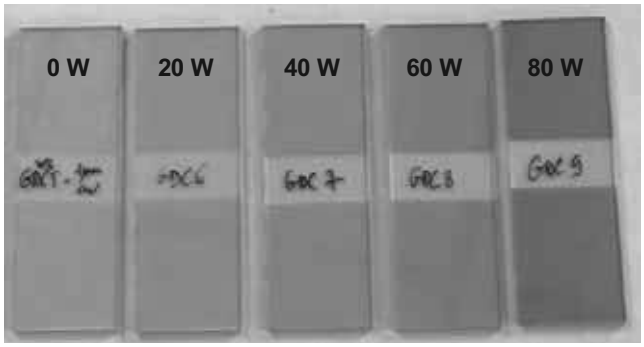

Figure 5. Pictures of GDC coatings as deposited on glass slides with different bias powers.

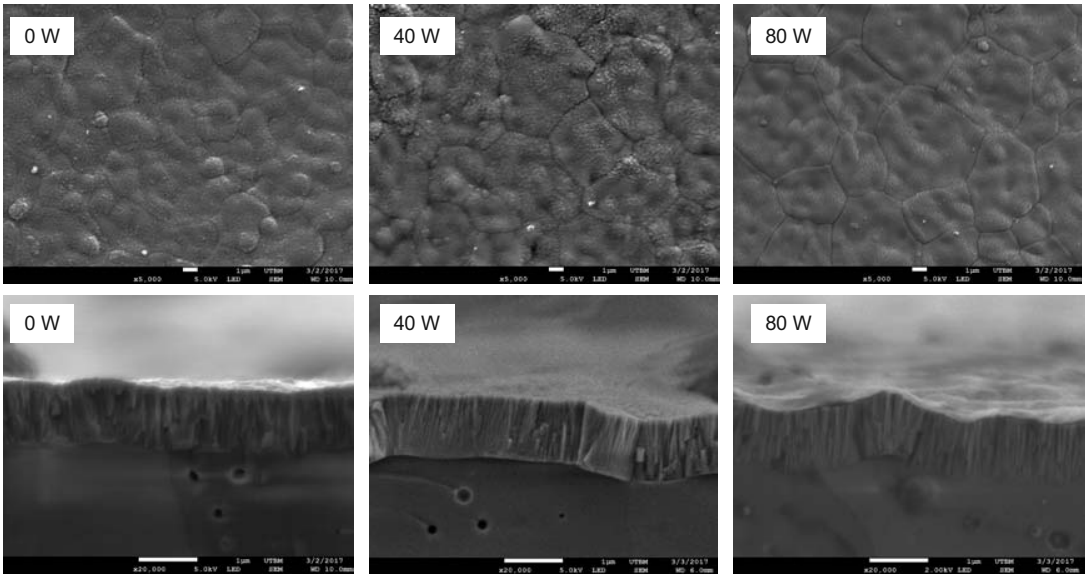

Figure 6. SEM view of surface and brittle fracture cross section of GDC coatings as deposited on 2R Cell substrate with different bias powers.

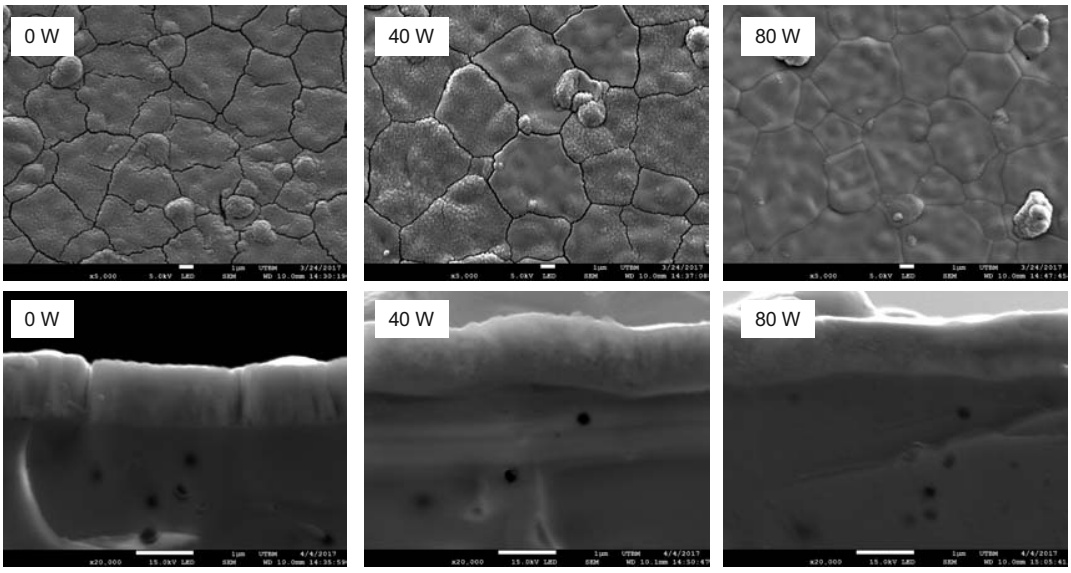

Figure 7. SEM micrographs of GDC coatings deposited on 2R Cell substrates under different bias powers after annealing at 1000°C for 2 h. Top view and brittle fracture cross section.

Figure 8 presents the X-ray diffraction spectra performed on as deposited GDC coatings deposited on 2R cell. As expected from previous studies, the as deposited coating presents the f.c.c. fluorite type structure of ceria with a rather fine microstructure, as shown by the full width at half maximum (FWHM) of the GDC characteristic diffraction lines [11]. The XRD pattern are indexed with the JCPDS card number 01-075-0161 and 01-082-1241 respectively for GDC and YSZ; the microstructure of the films refines with the increase of the bias power; it is a consequence of the increasing energy of impinging species. The diffraction line of (111) plane moves to a small angle induced by

the stress increase with the bias power. After annealing (Figure 9), no significant evolution of the FWHM was observed. However, a slight displacement of the diffraction lines of GDC towards higher angles can be observed, attributed to the stress relaxation of the coating and the oxygen content increase due to full oxidation. Indeed, due to the rather high M_T/M_G ratio, where M_T is the average mass of the target metal atoms and M_G the average mass of the gas phase, GDC deposited at low pressure are expected to be submitted to intense compressive stress [8].

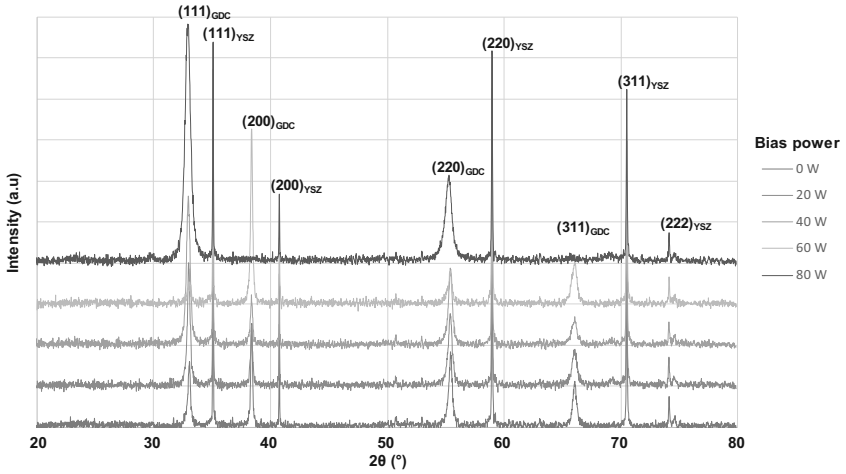

Figure 8. XRD patterns of as deposited GDC coating as function of bias power applied.

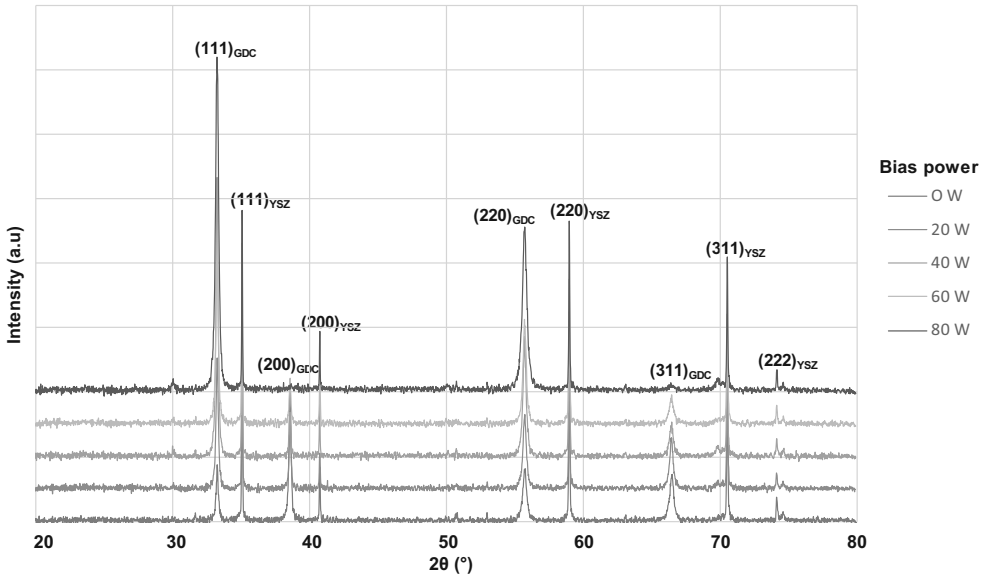

Figure 9. XRD patterns of annealed GDC coating as function of bias power applied (annealing condition: 2 h at 1000°C under static air).

I-V Curve Characterization

According to the morphological and structural features and the required properties for the buffer layer, only the coating deposited under 80 W substrate bias power was characterized in SOFC configuration. Before the cell introduction into the open flange set-up, a cathode is deposited on the GDC buffer layer using the screen printing method.

It is composed of 2 layers: the first one, the so-called composite layer, is made by 60 % of LSCF and 40 % of 20GDC. The second layer, the so-called current collection layer (CCL), is composed only by LSCF. Before printing the CCL, the composite layer was dried at 60ºC for 20 minutes (the same procedure was repeated after the deposition of the CCL). Finally, the cell was sintered in air at 1000ºC for 2h. The total cathode thickness is 18 µm.

Figure 11 shows the potential and power density versus current density of a 2R-Cell™ equipped with a GDC buffer layer deposited via reactive magnetron sputtering under 80 W substrate bias power. The OCV values are 1.143 V and 1.135 V respectively at the beginning and after 75 h running (decrease of only 0.7 %). The power density are 670 mW.cm^{-2} and 697 mW.cm^{-2} (0.8 A.cm^{-2}/790°C) respectively at experiment start and after 75 h. An improvement of 4 % is observed. No degradation was observed during the tested period (Figure 12); the cell voltage remains quite constant after 150 h, which confirms the interest of the GDC buffer layer realized by reactive magnetron sputtering.

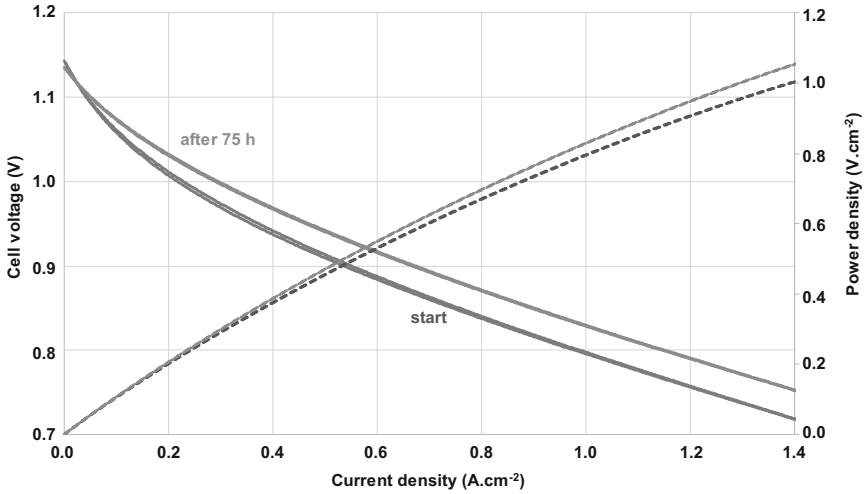

Figure 10. Potential and Power versus Current of a 2R-Cell™ equipped with a GDC buffer layer deposited via reactive magnetron sputtering under 80 W substrate bias power.

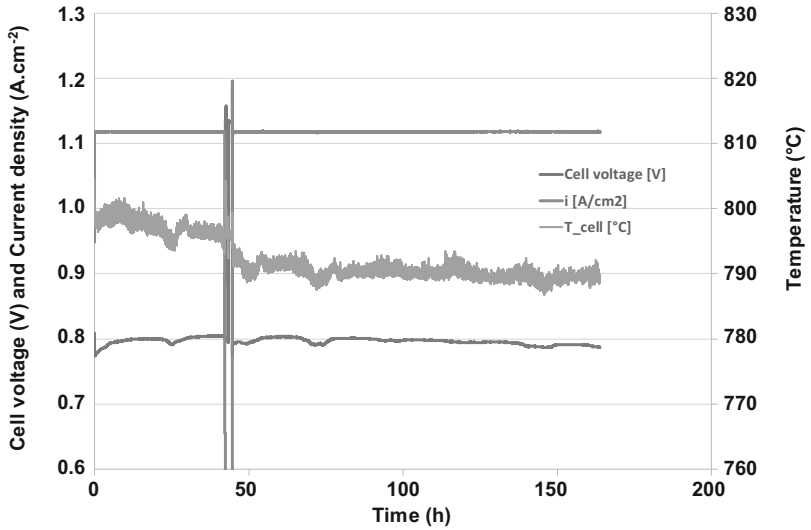

Figure 11. Cell potential at an operating temperature around 790°C recorded during 150 h.

Conclusions

In this work, the influence of bias power applied to the substrate holder of GDC coatings deposited by reactive magnetron sputtering has been studied. The application of PEM system could allow to obtain a relatively high sputtering rate, up to four times higher than without PEM system. It should be noted that increasing the bias power on the substrate leads to more and more compressive stress within the films and annealing treatment in the same condition that the cathode deposition relax these stresses. All coatings present f.c.c structure of ceria before and after thermal treatment. SEM observation reveals that 80 W substrate bias power allows adhesive coatings without cracks after annealing. According to previous work [5], GDC buffer layer increases the performance of the cell and no degradation is observe after 150 h.

Acknowledgments

This study is carried out within the framework of the European territorial cooperation program INTERREG V A France-Switzerland. It has benefited from financial support from the EU through the European Regional Development Fund (ERDF- € 139,176) and the Swiss Confederation's contribution of CHF 134,173.

References

1. E. Ivers-Tiffée, A. Weber, D. Herbstritt , *J. Eur. Ceram. Soc.*, **21**, 1805 (2001).
2. L. Qiu, T. Ichikawa, A. Hirano, N. Imanishi, Y. Takeda, *Solid State Ionics*, **158**, 55 (2003).
3. G. Constantin, C. Rossignol, P. Briois, A. Billard, L. Dessemond, E. Djurado, *Solid State Ionics*, **249-250**, 98 (2013).
4. K. Eguchi, T. Setoguchi, T. Inoue, H. Arai, *Solid State Ionics*, **52**, 165 (1992).
5. G. Di Domenicantonio, P. Briois, A. Billard and R. Ihringer, *ECS Trans.*, **57**(1), 867 (2013).
6. F. Perry, A. Billard, C. Frantz, *Surf. Coat. Technol.*, **94-95**, 681 (1997).
7. F. Perry, A. Billard, P. Pigeat, *Measurements*, **41(**5), 516 (2008).
8. F. Sanchette, T. Czerwiec, A. Billard, C. Frantz, *Surf. Coat. Technol.*, **96(**2-3), 184 (1997).
9. A. Billard, F. Perry, C. Frantz, *Surf. Coat. Technol.*, **94-95**, 345 (1997).
10. A. Billard, C. Frantz, *Surf. Coat. Technol.*, **59(**1-3), 41 (1993).
11. P. Briois, A. Billard, *Surf. Coat. Technol*., **201(**3-4), 1328 (2006).